Characteristics of Inclusions in Alloying Structural Steel during Refining

Ju Jiantao[1], Lv Zhenlin[1], Yang Shufeng[2]

[1]*School of Materials Science and Engineering, Xi'an University of Technology, Xi'an 710048, Shanxi, China*

[2]*School of Metallurgical and Ecological Engineering, University of Science and Technology Beijing, Beijing 100083, China*

Abstract

Systematic industrial experiments were carried out to investigate the characteristics of non-metallic inclusions with the aim of reducing their harmful effect on SAE4145 steel properties. Factsage thermodynamic software was used to simulate the conditions under which the inclusions occur. The number of inclusions in molten steel decreased rapidly with refining time. The inclusion morphology changed from an irregular initial shape to predominantly spherical inclusions. After vacuum treatment, almost all of the inclusions were CaO-SiO_2-Al_2O_3-MgO composites. To form low melting point inclusions of CaO-SiO_2-20%Al_2O_3-MgO, the corresponding activities of [O], [Ca], [Mg] and [Al] should be controlled in the range of $a_{[O]}$ 0–10 ppm, $a_{[Ca]}$ 0–45×10^{-10} ppm, $a_{[Mg]}$ 0–0.3 ppm, and $a_{[Al]}$ 0~20 ppm.

Keywords: *alloying structural steel; non-metallic inclusions; ladle furnace-vacuum degassing; thermodynamic*

1. Introduction

SAE4145 is an alloying structural steel often used for engine crankshafts. Because of the severe conditions under which they operate, such as dynamic loads, high torque, alternating bending stress, and long-term high-speed running, crankshafts are often destroyed by torsional vibration, bending deformation and even fatigue fracture [1]. Thus, higher fatigue strength, impact toughness, and wear resistance are required in the crankshafts [1-4]. Numerous studies [5-9] show that fatigue is the dominant mechanism for crankshaft failure and fatigue cracks are likely to initiate from non-metallic inclusions [10]. The detrimental effect of inclusions depends on the difference between the thermal expansion coefficient of the inclusion and that of the steel matrix. Hard, large, brittle, and un-deformable inclusions should be avoided, because they cannot be deformed with the steel matrix during hot rolling and could result in stress concentrations at the steel/inclusion interface [11].

Many studies have been carried out on the characteristics of steel inclusions, such as spring, bearing, hot work die steel, tire cord, gear, and electrical steel [12-15]. These studies [11] show that inclusions with a low melting point and good plasticity can be formed by controlling the deoxidant alloys (or a mixture of deoxidant and flux), the synthetic top slag and/or the flux injection. However, no reports exist on the characteristics of SAE4145 steel inclusions.

In this paper, industrial experiments were carried out to investigate systematically the characteristics of non-metallic inclusions during ladle furnace-vacuum degassing (LF-VD) refining. Furthermore, discussions are presented on the formation conditions of the desired inclusions, which were based on the thermodynamic equilibrium between the steel and the inclusions.

2. Experimental

In this work, the experimental steel is SAE4145 with a composition (wt.%) of C 0.45, Si 0.20, Mn 0.80, P 0.02, S 0.008, Mo 0.15, Cu 0.07, and Cr 0.94. The process to produce SAE4145 is as follows: 50 t electric arc furnace (EAF) → 50 t LF-VD → CaSi treatment → Continuous Casting The LF refining time is approximately 75 min and the VD treatment time is 70 min.

Steel samples were taken during four different runs at different refining stages, such as before LF refining (Sample 1), in the middle of LF refining (Samples 2 and 3), at the end of LF refining (Sample 4), and at the end of VD (Sample 5). During sampling, the samplers were immerged in the molten steel 300 mm below the bath surface. Inclusions were observed and analyzed using scanning electron microscopy-energy dispersive spectroscopy. The total oxygen content (T[O]) was determined using the GALILEO ON/H analyzer.

3. Results and discussion

3.1 Total oxygen and amount of inclusions

Figure 1 shows the change in total oxygen content and amount of inclusions during LF-VD refining. The T[O] content decreased from 260 to 10 ppm and the amount of non-metallic inclusions in the molten steel decreased rapidly with refining time. The removal rate over the entire refining process was 88.8%, which indicates that the LF-VD process is able to remove oxide inclusions.

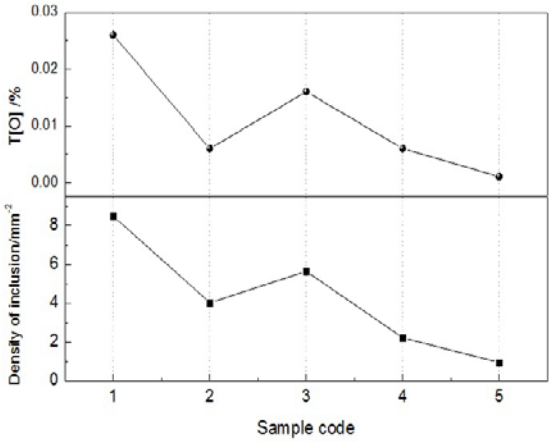

Figure 1 Change in T[O] and amount of inclusions during LF-VD refining

3.2 Morphology and composition of typical inclusions

The morphologies of typical inclusions in each sample are shown in Figs 2–6 with inclusion compositions listed in Table 1.

As shown in Fig. 2 (a), irregular cluster-like inclusions of alumina or spinel were observed in Sample 1. Figure 2 (b) shows other typical inclusions that are rectangular in shape. Large amounts of Al_2O_3 formed with the addition of deoxidizers like aluminum, ferrosilicon, and ferromanganese after EAF tapping. Meanwhile, in the FeO-SiO_2-Al_2O_3-MnO system, complex inclusions containing less CaO were formed by a reaction of the deoxidation products (SiO_2, Al_2O_3, MnO) and high oxide slags.

As can be seen in Fig. 3, the Al_2O_3 inclusions were encased in complex inclusions. The inclusion shape changed from irregular to ellipsoidal. During the first stage of LF refining, the basicity of the slag was in the range of 2.0–2.5 and the oxygen content in the steel reached up to 50 ppm. The low basicity and high SiO_2 content could result in the coexistence of both Al_2O_3 and Ca-Si-Mn-Mg-O inclusions with higher Si and/or lower Al content.

Figure 4 shows the morphologies of the CaO-SiO_2-Al_2O_3-MgO inclusions in Sample 3. The formation mechanism of these inclusions is explained as follows. After Al-deoxidization, a great number of Al_2O_3 inclusions formed in the steel melt. As the refining process progressed, the Mg content in the steel increased, possibly because of the erosion of magnesia carbon brick by a chemical reaction (1). However, because of the low level of FeO content in the slag, alumina inclusions are unstable even when low levels of Ca exist in the steel. Ca could be reduced from the slag by reaction (2). The Mg activity was higher than that of Ca and the Al_2O_3 inclusions formed would react with dissolved Mg and change into MgO-Al_2O_3 system inclusions, as expressed by reaction (3). The formed MgO-Al_2O_3 is not stable when Ca enters the steel and would be transformed into calcium aluminates by reaction (4) and surround the original MgO-Al_2O_3 inclusion core [16].

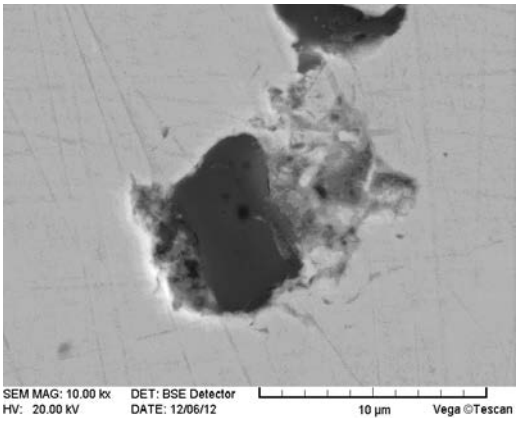

a)

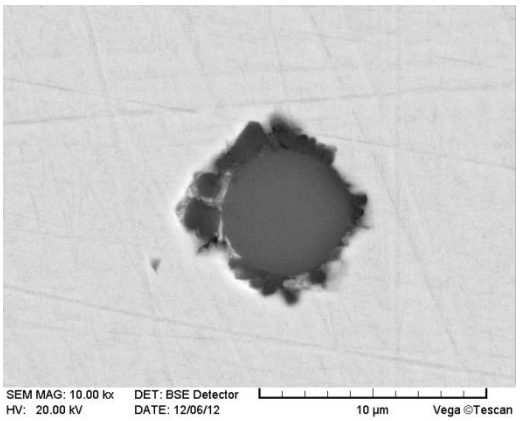

b)

Figure 2 Morphologies of a typical inclusion in Sample 1

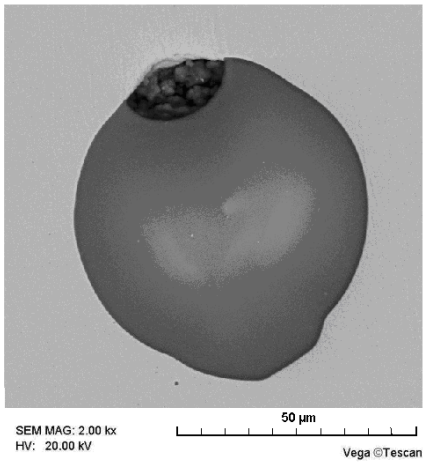

Figure 3 Morphologies of CaO-SiO_2-MnO-MgO inclusions in Sample 2

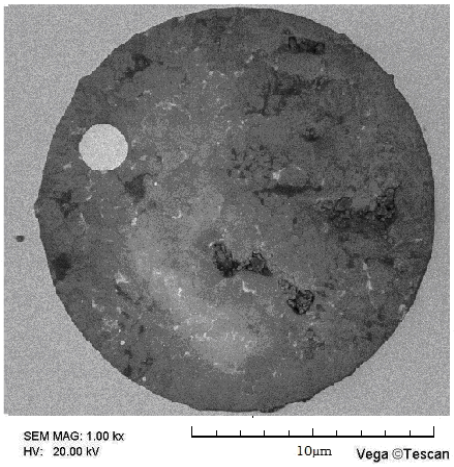

Figure 4 Morphologies of CaO-SiO_2-Al_2O_3-MgO inclusions in Sample 3

Typical inclusions found after LF refining in Sample 4 are displayed in Fig. 5. With time, MnO disappears from the inclusions while the content of CaO increases. Thereafter, most inclusions are CaO-Al_2O_3-SiO_2-MgO.

$$3(MgO) + 2[Al] = (Al_2O_3) + 3[Mg] \quad (1)$$

$$3(CaO) + 2[Al] = 3[Ca] + (Al_2O_3) \quad (2)$$

$$[Mg] + n/3(Al_2O_3) = (MgO\cdot(n-1)/3Al_2O_3) + 2/3[Al] \quad (3)$$

$$x[Ca] + (yMgO\cdot zAl_2O_3) = (xCaO\cdot(y-x)MgO\cdot zAl_2O_3) + x[Mg] \quad (4)$$

As shown in Fig. 6, after vacuum treatment, almost all inclusions were CaO-SiO_2-Al_2O_3-MgO with highest CaO and lower Al_2O_3 content. The MgO content in the inclusions was close to that of the furnace lining. In VD refining, the oxygen and sulfur content is reduced further by vacuum degassing and stirring with Ar. However, the furnace lining is eroded under the high basicity, low oxygen, and high vacuum conditions. Most of the alumina can be floated and captured by the top slag, while some complex inclusions remain in the liquid steel formed by the interaction of CaO, SiO_2, MgO, and a small amount of fine residual Al_2O_3.

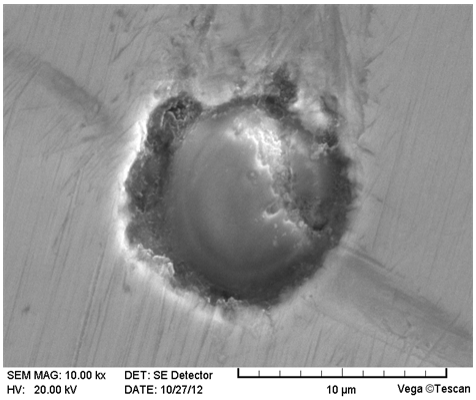

Figure 5 Morphologies of typical CaO-SiO_2-Al_2O_3-MgO inclusions in Sample 4

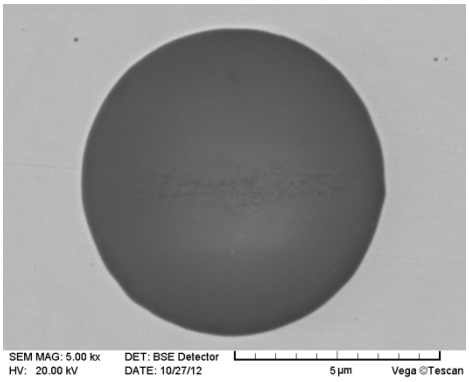

Figure 6 Morphologies of typical CaO-SiO_2-Al_2O_3-MgO inclusions in Sample 5

Table 1 Inclusion compositions/wt%

Code	Morphology	Location	O	Al	Si	Ca	Mg	Mn	Fe
1-a	Irregular		10.56	84.07					5.37
1-b	Rectangular		8.50	32.28	23.67	3.55		16.43	4.06
2	Ellipsoidal	3	8.53	4.50	34.18	31.98	6.07	13.06	1.67
3	Spherical	1	40.06	19.05	9.54	31.36			
4	Spherical		21.42	10.73	19.27	41.65	3.70		3.19
5	Spherical	1	5.20	3.47	20.59	57.87	6.35		2.56

3.3 Thermodynamic calculation of optimization

Because residual inclusions in steel are unavoidable and brittle and undeformable inclusions are undesirable, it is important to modify the inclusions into liquid inclusions in the molten steel [17]. Previous reports show that when the inclusion melting point is below 1673 K, good deformation ability is exhibited in the rolling process [14]. In this paper, Factsage software was used to calculate equilibrium and phase diagrams with the liquid zone in the CaO-SiO_2-Al_2O_3-MgO system under 1873 K and the activities of CaO, SiO_2, and MgO calculated by Factsage. The activities of Ca, Mg, Al, and O in the liquid steel bath were computed in equilibrium with inclusions. The soluble aluminum content in the steel is 0.03% at 1873 K.

Iso-activity lines of MgO, CaO, and SiO_2 in the liquid zone are shown in Fig. 7. Regions enclosed by heavy lines and short dot lines represent the liquid zones of 1873 and 1673 K, respectively. To obtain CaO-SiO_2-20%Al_2O_3-MgO system inclusions with a low melting point under 1673 K, the chemical composition (mass percent) of inclusions should be controlled in the region with MgO and CaO (mass percent) lower than 24% and 40%, respectively, and SiO_2 (mass percent) between 32% and 68%. Accordingly, the activities should be: MgO from 0.001 to 0.1, CaO from 0.00001 to 0.01, and SiO_2 greater than 0.05.

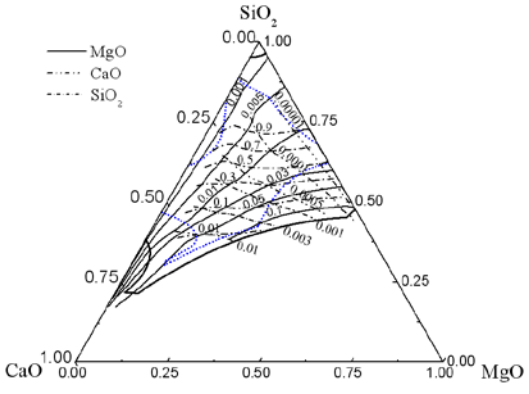

Figure 7 Iso-a_{MgO}, iso-a_{CaO}, and iso-a_{SiO2} lines in the liquid zone of the CaO-SiO_2-20%Al_2O_3-MgO system

Equilibrium activities of Ca, Mg, Al, and O in steel were calculated and are shown in Fig. 8. The region enclosed by heavy lines is the liquid zone (≤ 1873 K) and the lines with figures within the liquid zone are the iso-activity lines of [Ca], [Mg], [Al], and [O]. The activities of Ca and Mg increase with an increase in CaO and MgO content in the inclusions. However, the Al and O activities decrease with an increase in SiO_2 content in the inclusions. At 1873K and 0.03% (mass percent) soluble aluminum in steel, to form low melting point inclusions, the activities of [O], [Ca], [Mg], and [Al] should be in the following ranges: a[O]: 0–10 ppm, $a_{[Ca]}$: 0–45×10^{-10} ppm, $a_{[Mg]}$: 0–0.3 ppm, and $a_{[Al]}$:0–20 ppm.

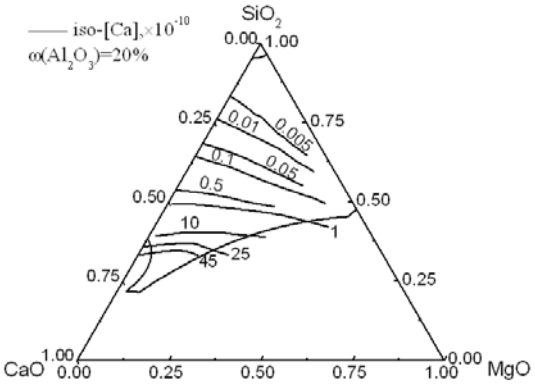

a)

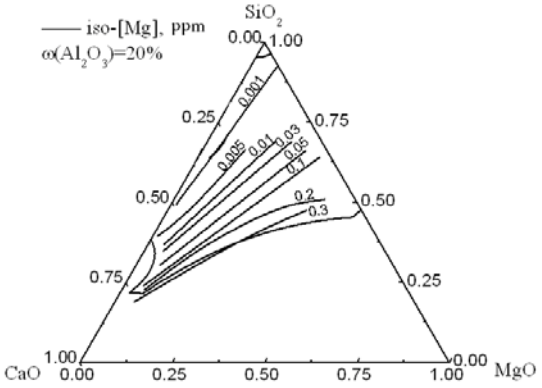

b)

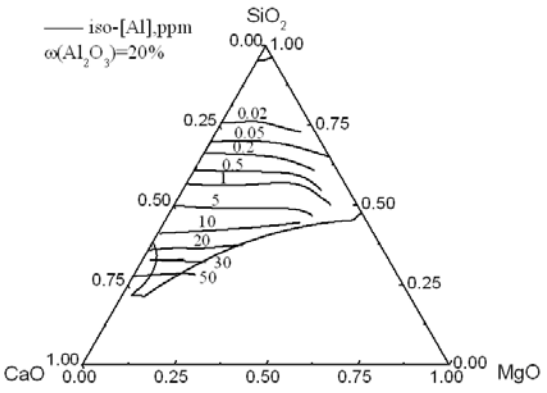

c)

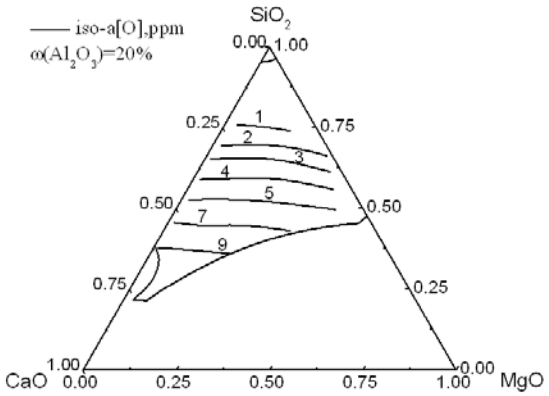

d)

Figure 8 Iso-$a_{[Ca]}$, iso-$a_{[Mg]}$, iso-$a_{[Al]}$, and iso-$a_{[O]}$ lines in the liquid zone of the CaO-SiO_2-20%Al_2O_3-MgO system

Conclusions

The number of inclusions in molten steel decreases rapidly with refining time. The inclusion morphology changes from irregularly shaped to predominantly spherical. After vacuum treatment, almost all inclusions were smaller-sized CaO-SiO_2-Al_2O_3-MgO.

To obtain CaO-SiO_2-20%Al_2O_3-MgO inclusions with low melting point, their chemical composition should be controlled as follows: MgO and CaO (mass percent) should be present at less than 24% and 40%, respectively, and SiO_2 (mass percent) between 32% and 68%. The activities should be: MgO from 0.001 to 0.1, CaO from 0.00001 to 0.01, and SiO_2 greater than 0.05.

To form low melting point inclusions, the corresponding activities of [O], [Ca], [Mg], and [Al] should be controlled in the following

ranges: $a_{[O]}$: 0–10 ppm, $a_{[Ca]}$: 0–45×10^{-10} ppm, $a_{[Mg]}$: 0–0.3 ppm, and $a_{[Al]}$:0–20 ppm.

Acknowledgments

The authors are grateful for support from the National Science Foundation China (grant no.51304016 and 51074021)

References

1. FENG Ji-jun, GUO Wen-fang. Main Failure Forms and Analysis of Automobile Engine Crankshaft [J] Failure Analysis and Prevention, 2006,1 (02) :7-12.

2. ESPADAFOR F J, VILLANUEVA J B, GARCÍA M T. Analysis of a Diesel Generator Crankshaft Failure [J]. Engineering Failure Analysis, 2009, 16(7): 2333-2341.

3. YU Zhi-wei, XU Xiao-lei. Failure Analysis of a Diesel Engine Crankshaft [J]. Engineering Failure Analysis, 2005, 12(3): 487–495.

4. CHEN Shu-hao, MIN Jiang, HE Xiao-fei, et al. Top Slag Refining for Inclusion Composition Transform Control in Tire Cord Steel[J]. International Journal of Minerals Metallurgy and M, 2012, 19(6): 490-498.

5. ZHU Hua-ming, LIU Jun-feng, LIU Fu-xu. Failure Analysis of Engine Crankshaft [J]. Foreign Heat Treatment of Metals, 2002, 23 (02): 45-46.

6. DONG Shi-yun, SHI Chang-liang, XU Bin-shi, et al. Failure Analysis of Crankshaft in a Heavy-duty Vehicle Engine [J]. Failure Analysis and Prevention, 2009, 4(03):138-142.

7. WANG Yan-rong, DIAO Zhan-ying, CHI Shao-ning, et al. Failure Analysis on Early Fatigue Cracking of Engine Crankshaft [J]. PTCA (PART A: PHYS.TEST.), 2011, 47 (6):388-391.

8. Murakami Y. Mechanism of Fatigue Failure in Ultralong Life Regime and Application to Fatigue Design [J]. Fatigue and Fracture of Engineering Materials and Structures, 2002, 15:2927~2938.

9. Wang Q Y，Zhang H，Sriraman M R，et al. Very Long Life Fatigue Behavior of Bearing Steel AISI 52100[J]. Key Engineering Materials，2005，297~300:1846~1851.

10. Wang Q Y，Berard J Y，Dubarre A，et al. Gigacycle Fatigue of Ferrous Alloys [J]. Fatigue and Fracture of Engineering Materials and Structures, 1999，22:667~672.

11. LUO Chun-hui. Modeling the Behavior of Inclusions in Plastic Deformation of Steels [D]. Stockholm: KTH Superseded Departments, Production Engineerin, 2001: 31.

12. WANG Chun-qiong, LI Chang-rong. Behavior of Non-metallic Inclusion of H13 Steel in LF-VD Refining Process [J]. Die&Mould industry, 2011,37(6):63-66.

13. ZHANG Li-heng, WANG Guo-cheng, ZHU Qing-de. Thermodynamic Analysis Formed by Non-metallic Inclusions in Welding Gas Vessel Steel HP295 [J]. Nonferrous Metals Science and Engineering, 2011, 2(6): 22-28

14. ZHANG Bo, WANG Fu-ming, LI Chang-rong. Thermodynamic Calculations on Low Melting Point Area of SiO2-Al2O3-CaO-MgO Inclusion and its Control [J]. Iron and Steel, 2011, 46(1):39-44.

15. Yu TANG. Effect of Slag Composition on Inclusion Control in LF-VD Process for Ultra-low Oxygen Alloyed Structural Steel [J]. Procedia Earth and Planetary Science 2011, 2:89-97.

16. JIANG Min, WANG Xin-hua, CHEN Bin, et al. Laboratory Study on Evolution Mechanisms of Non-metallic Inclusions in High Strength Alloyed Steel Refined by High Basicity Slag[J]. ISIJ International, 2010, 50 (1): 95–104.

17. YOUN-BAE K, HAE-GEON L. Inclusions chemistry for Mn/Si Deoxidized Steels: Thermodynamic Predictions and Experimental Confirmations [J]. ISIJ International, 2004, 44(6): 1006-1015.